Submitted to the
XXII International Symposium on Lepton-Photon Interactions at High Energy
30 June - 5 July, Uppsala, Sweden

Abstract: 258 **Session: EW&B**

Search for stop production in R-parity-violating supersymmetry at HERA

ZEUS Collaboration

Abstract

A search for stop production in R-parity-violating supersymmetry has been performed with the ZEUS detector at HERA using an integrated luminosity of 65.5 pb^{-1} of e^+p collision data. The resonant production of stop via an R-parity-violating Yukawa coupling, λ'_{131}, where the subscript denotes generation indices, was considered. Both the decay via λ'_{131}, $\tilde{t} \to e^+d$, and the gauge R-parity-conserving decay, $\tilde{t} \to b\chi^+$, were taken into account. No evidence for stop production was found and limits were set on λ'_{131} as a function of the stop mass in the framework of the Minimal Supersymmetric Standard Model.

1 Introduction

The electron-proton collider HERA is an ideal place to search for possible exotic states originating from electron-quark fusion. Such new states naturally arise in grand unification theories that arrange quarks and leptons in common multiplets (as leptoquarks) [1] or in supersymmetric models that violate R-parity (as squarks) [2]. Scalar or vector leptoquark states have been intensively searched for by the ZEUS Collaboration [3]. This paper presents a search in e^+p collisions for the stop-squark, the scalar partner of the top quark, which is expected to be the lightest squark.

In e^+p collisions, the stop can be resonantly produced by the fusion of the positron and d-quark in the proton, $e^+d \rightarrow \tilde{t}$, via an R-parity-violating Yukawa coupling λ'_{131} (where the subscripts are generation indices) [2]. The decay leads to a rich topology since, beside the R-parity-violating channel, $\tilde{t} \rightarrow e^+d$, there is a number of possible gauge decays leading to final states with multi-jets and one or more leptons. In the present paper final states involving one positron and one (e-J) or more jets (e-MJ) and one neutrino and multi-jets (ν-MJ) were studied. The branching ratio of the different topologies depends on the SUSY scenario, therefore, a scan over a wide range of SUSY parameters was performed.

The analysis presented in this paper uses e^+p data collected by the ZEUS detector in 1999 and 2000, corresponding to an integrated luminosity of 65.5 pb^{-1}. Similar searches for squark production at HERA have been performed by the H1 Collaboration [4, 5].

2 SUSY phenomenological backgrounds

The results were interpreted in the framework of the R-parity-violating Minimal Supersymmetric Standard Model (MSSM) [2], where the masses of the neutralinos, charginos and gluinos are determined by the following MSSM parameters: the mass term μ, which mixes the Higgs superfields, the soft SUSY-breaking parameters M_1, M_2 and M_3 for the $U(1)$, $SU(2)$ and $SU(3)$ gauginos, respectively, and $\tan\beta$, the ratio of the vacuum expectation values of the two neutral scalar Higgs fields. The masses of the first- and second-generation squarks and all the sleptons have been set to 1 TeV. The mass of the lighter stop[1] was varied in the range $100 - 280$ GeV.

In order to reduce the number of free parameters, the following additional assumptions were made:

[1] The partners of the left- and right-handed top, $\tilde{t}_L$ and $\tilde{t}_R$, mix together in two mass eigenstates, $\tilde{t}_1$ and $\tilde{t}_2$, which are strongly non-degenerate due to the large top mass. Throughout this paper, the lighter stop is given by the symbol $\tilde{t}$.

- along all the R-parity-violating couplings (λ_{ijk}, λ'_{ijk} and λ''_{ijk}, where i, j, k are generation indices), only the Yukawa coupling λ'_{131} was assumed to be non-zero;
- the χ_1^0 was required to be the lightest supersymmetric particle (LSP) and SUSY scenarios where a χ_1^0 is lighter than 35 GeV were not considered, as they are already excluded by LEP results [6];
- a common mass ($M_{1/2}$) was assumed for all gauginos at the GUT scale. This leads to the usual relations [7] for M_1, M_2 and M_3;
- the gluino, the SUSY partner of the gluon, was assumed to be heavier than $\tilde{t}$, so that the decay $\tilde{t} \to t\ \tilde{g}$ was kinematically forbidden.

The signal cross sections have been evaluated using the narrow width approximation (NWA) at leading order in QCD, corrected for the effect due to the initial-state positron radiation. The signal efficiency for the stop gauge decays was estimated using the program SUSYGEN [8]. For each SUSY scenario (μ, M_2, tanβ), branching ratios of the stop were calculated and the detector efficiency was obtained using simulated events. The gauge stop decay, $\tilde{t} \to \tilde{\chi}_1^+ b$, was considered with subsequent R-parity-violating ($\tilde{\chi}_1^+ \to e^+ \overline{b} d$) or gauge ($\tilde{\chi}_1^+ \to \tilde{\chi}_1^0 W^+$, $\tilde{\chi}_1^0 \to \nu_e \overline{b} d$, $W^+ \to qq'$) chargino decay. In addition the R-parity-violating stop decay ($\tilde{t} \to e^+ d$) was simulated using PYTHIA [9].

3 Event selection

The signal events are expected to be characterised by a high-energy lepton in the final state. In the case of a positron in the final state (e-J and e-MJ channels), the trigger selection was based on a standard neutral current (NC) trigger used in searches for resonance states decaying in eq [3] and in NC deep inelastic scattering (DIS) studies [10]. For the neutrino case (ν-MJ channel), the same trigger selection as used in the ZEUS charged current (CC) DIS analysis was used [11].

The signal-search procedure was performed in two steps. Initially, different pre-selections are applied to select NC and CC events. Finally, more restrictive selections, designed to optimize the signal sensitivity, were applied.

3.1 NC pre-selection

The following conditions were designed to select a sample of high-Q^2 NC events, some of which were also used at the trigger level with a lower threshold.

- Z-coordinate of the event vertex compatible with an ep interaction, $|Z_{\text{vtx}}| < 50$ cm;

- a high-energy positron reconstructed combining both calorimeter and tracking information [12]. A positron energy $E_e > 8$ GeV was required. This cut was increased to $E_e > 20$ GeV for very forward positrons ($\theta_e < 0.3$, where θ_e is the positron polar angle) that are outside the acceptance of the central tracking detector;

- $50 < \sum_i (E - P_Z)_i < 65$ GeV, where the sum runs over the final state positron and all the other calorimeter energy deposits. For NC DIS events, where only particles in the very forward direction escape detection, $E - P_Z \sim 2E_e^{\rm beam} = 55$ GeV, where $E_e^{\rm beam}$ is the positron beam energy;

- $Q^2_{\rm DA} > 1000$ GeV^2 and $0.2 < y_{\rm DA} < 0.98$, where $Q^2_{\rm DA}$ and $y_{\rm DA}$ are the usual DIS kinematic variables reconstructed using the polar angles of the positron and of the hadronic system [13]. The above conditions were imposed in order to restrict the search to a region where the signal is enhanced with respect to NC DIS and the reconstruction of the kinematic variables is reliable;

- $M_{eX} > 100$ GeV, where M_{eX} is the invariant mass of the positron and the hadronic system evaluated using the following relation that exploits longitudinal and transverse momentum conservation:

$$M^2_{eX} = 2E_e^{\rm beam} \sum_i (E + P_Z)_i, \qquad (1)$$

  where E and P_Z are the energy of the calorimeter deposits and its z-projection. The sum runs over the final state positron and all the other energy deposits having a polar angle > 0.1 rad, to exclude the proton remnant.

The mean and resolution of the reconstructed mass were evaluated using the signal Monte Carlo (MC). The mean is slightly overestimated at low masses (3% at 100 GeV), while the agreement improves towards high masses ($< 1\%$ above 150 GeV). The resolution is between 5% and 1.5% in the mass range $100 - 300$ GeV. After the pre-selection cuts 2045 events survived, in good agreement with the expectation of the standard model Monte Carlo (SM MC), 2093 ± 10. The SM prediction is dominated by the NC DIS. This process was simulated using the DJANGO 6 [14] program interfaced to ARIADNE [15] to model the QCD cascade.

Figure 1 shows the distributions of the energy of the scattered positron, E'_e, $y_{\rm DA}$, $\log_{10}(Q^2_{\rm DA}/{\rm GeV}^2)$ and the ratio of the transverse momentum and transverse energy $P_{t,{\rm had}}/E_{t,{\rm had}}$ for data and MC; reasonable agreement between data and MC is seen for all variables.

3.2 CC pre-selection

Events with a neutrino in the final state have a topology similar to CC DIS. The following selection cuts were applied in order to select a sample of high-Q^2 CC events and suppress the non-ep contribution.

- Z-coordinate of the event vertex compatible with an ep interaction, $|Z_{\rm vtx}| < 50$ cm;
- no reconstructed positron satisfying the same criteria used in NC pre-selection;
- high missing transverse momentum, P_t >20 GeV;
- $0.4 < y_{\rm JB} < 0.95$, where $y_{\rm JB}$ is reconstructed using the Jacquet-Blondel method [16].
- $M_{\nu X} > 80$ GeV, where $M_{\nu X}$ is the invariant mass of the hadronic system evaluated using the following relation that exploits longitudinal and transverse momentum conservation:

$$M_{\nu X}^2 = 2E_e^{\rm beam}\left(\sum_i (E+P_z)_i + P_t^2/(2E_e^{\rm beam}\,(1-y_{\rm JB}))\right), \qquad (2)$$

  where E and P_Z are the energy of the calorimeter deposits and its Z-projection. The sum runs over all the calorimeter energy deposits having a polar angle > 0.1, to exclude the proton remnant.

The mass resolution is between 10% and 3% in the mass range $100 - 300$ GeV. The mean mass is slightly underestimated at high masses (1.5% at 300 GeV), while the agreement improves towards low masses ($<$ 1% above 120 GeV). After the CC pre-selection cuts 262 events survived, in good agreement with the expectation of the SM MC, 254 ± 3. The SM prediction is dominated by CC DIS, with a small contribution coming from photoproduction processes. CC DIS was simulated using the LEPTO 6.5 [17] program which uses the matrix element plus parton shower (MEPS) to model the QCD cascade.

Figure 2 shows the distributions of P_t, $y_{\rm JB}$, $\log_{10}(Q^2_{\rm JB}/{\rm GeV}^2)$ and P_t/E_t for data and MC; reasonable agreement is achieved for all the variables.

3.3 Final selection

No signal was observed. Therefore, the final selection was optimised to be maximally sensitive to the stop production cross section. For the channels with a final-state positron, the following cuts were imposed:

- $Q^2_{\rm DA} > 3000$ GeV^2;
- the y cut was tuned along the reconstructed mass, $y_{\rm DA} > 0.8 - 0.2$, in the mass range $100 - 300$ GeV.

Finally, a $P_{t,\mathrm{had}}/E_{t,\mathrm{had}}$ cut $>(<)$ 0.8 is used to enrich the sample of one jet (multi-jets) events. For the CC channel, the following requirements were applied:

- $y_{\mathrm{JB}} > 0.42$, which corresponds to $E - P_z > 25$ GeV;
- $P_t/E_t < 0.4$.

Final cut values, numbers of events from data and MC SM and signal efficiency are summarized in Table 1.

Figure 3 shows the comparison between data and MC for mass distributions after the pre-selection and final selection for the different channels; good agreement is observed in all the distributions.

4 Systematic checks

The following sources of systematic uncertainty in the SM predictions were taken into account:

- uncertainty in the PDFs input to NC and CC DIS cross sections, evaluated using the procedure suggested by the CTEQ group [18];
- uncertainty related to the knowledge of the calorimeter energy scale, $\pm 1\%$ ($\pm 2\%$) for the electromagnetic (hadronic) section;
- uncertainty in the integrated luminosity measurement, $\pm 2.25\%$.

In addition, the following uncertainties related to the signal simulation were considered:

- the uncertainties in the signal efficiency due to interpolation between different SUSY scenarios was $\simeq 15\%$;
- the theoretical uncertainty on the signal cross section due to the uncertainty in the d-quark parton density [18].

5 Results

Since no evidence for e-J, e-MJ and ν-MJ resonances was found, 95% confidence level (CL) upper limits on λ'_{131} as a function of the stop mass were evaluated. A scan of the mass spectrum in 1 GeV steps was performed using a sliding window of width[2] $\pm(2-4)\sigma_{M_{\ell X}}$ ($\ell = e$ or ν). At each stop mass, the 95% CL on λ'_{131} was evaluated using the data events, the SM predictions and the signal efficiencies for the considered mass window.

[2] The mass window width was also optimized to increase the signal sensitivity.

A Bayesian approach assuming a flat prior for the signal cross section was used. The systematic uncertainties were taken into account in the limit setting. Figure 4 shows the 95% CL limit on λ'_{131} as a function of the stop mass for a range of μ (from -300 GeV to 300 GeV in steps of 20 GeV), M_2 (from 100 GeV to 300 GeV in steps of 10 GeV) and $\tan\beta = 6$. The limits for masses up to 250 GeV improve on the low-energy limits from atomic parity violation (APV) measurements (dashed line) [2] and depend weakly on the different SUSY scenarios. The H1 collaboration obtained similar constraints [4] using similar SUSY scenarios.

6 Conclusions

A search for stop production in e^+p collisions at HERA was performed using an integrated luminosity of 65.5 pb^{-1} collected by the ZEUS detector in 1999-2000 data taking. No evidence for resonances in the decay channels with jet(s) and one high-P_t lepton was found. The results have been interpreted in the framework of the R-parity-violating MSSM, setting constraints on the Yukawa coupling λ'_{131} as a function of the stop mass. The constraints, evaluated for a wide range of the MSSM parameters μ and M_2, exhibit a weak dependence on the different SUSY scenarios and improve on limits from low-energy APV measurements for stop masses lower than 250 GeV.

References

[1] W. Buchmüller, R. Rückl and D. Wyler, Phys. Lett. **B 191**, 442 (1987). Erratum in Phys. Lett. **B 448**, 320 (1999).

[2] H.K. Dreiner, *Perspectives on Supersymmetry*, Ed. by G.L. Kane, World Scientific, hep-ph/9707435.

[3] ZEUS Coll., S. Chekanov et al., Phys. Rev. **D 68**, 052004 (2003).

[4] H1 Coll., A. Aktas et al., Eur. Phys. J. **C 36**, 425 (2004).

[5] H1 Coll., A. Aktas et al., Phys. Lett. **B 599**, 159 (2004).

[6] L3 Coll., M. Acciarri et al., Eur. Phys. J. **C 19** 397 (2001).

[7] N. Polonsky *Supersymmetry: Structure and Phenomena*, hep-ph/0108236.

[8] N. Ghodbane, S. Katsanevas, P. Morawitz and E. Perez, *SUSYGEN 3.* hep-ph/9909499.

[9] T. Sjöstrand, Comput. Phys. Commun. **82**, 74 (1994).

[10] ZEUS Coll., S. Chekanov et al., Phys. Rev. **D 70**, 052001 (2004).

[11] ZEUS Coll., S. Chekanov et al., Eur. Phys. J. **C 32**, 16 (2003).

[12] ZEUS Coll., J. Breitweg et al., Z. Phys. **C 74**, 207 (1997).

[13] S. Bentvelsen, J. Engelen and P. Kooijman, *Proc. of the Workshop on Physics at HERA*, W. Buchmüller and G. Ingelman (eds.), Vol 1, p.23. Hamburg, Germany, DESY (1992).

[14] K. Charchula, G.A. Schuler and H. Spiesberger, Comput. Phys. Commun. **81**, 381 (1994).

[15] L. Lönnblad, Comput. Phys. Commun. **71**, 15 (1992).

[16] F. Jacques and A. Blondel, *Preceedings of the Study for an ep Facility for Europe.* U. Amaldi (ed.), p. 391. Hamburg, Germany (1979).

[17] G. Ingelman, A. Edin and J. Rathsman, Comput. Phys. Commun. **101**, 108 (1997).

[18] CTEQ Coll., H.L. Lai et al., Phys. Rev. **D 55**, 1280 (1997).

Decay channel	y	$P_{t,\mathrm{had}}/E_{t,\mathrm{had}}$	Data	MC SM	Signal ϵ
e-J	$> 0.8 - 0.002 \cdot M_{eX}$	> 0.8	97	88.5	0.2-0.55
e-MJ	$> 0.8 - 0.002 \cdot M_{eX}$	< 0.8	90	93.8	0.25-0.5
ν-MJ	> 0.42	< 0.4	8	9.9	0.1-0.4

Table 1: *Summary of final selection cuts, number of observed and expected events and signal efficiencies for the different stop final states.*

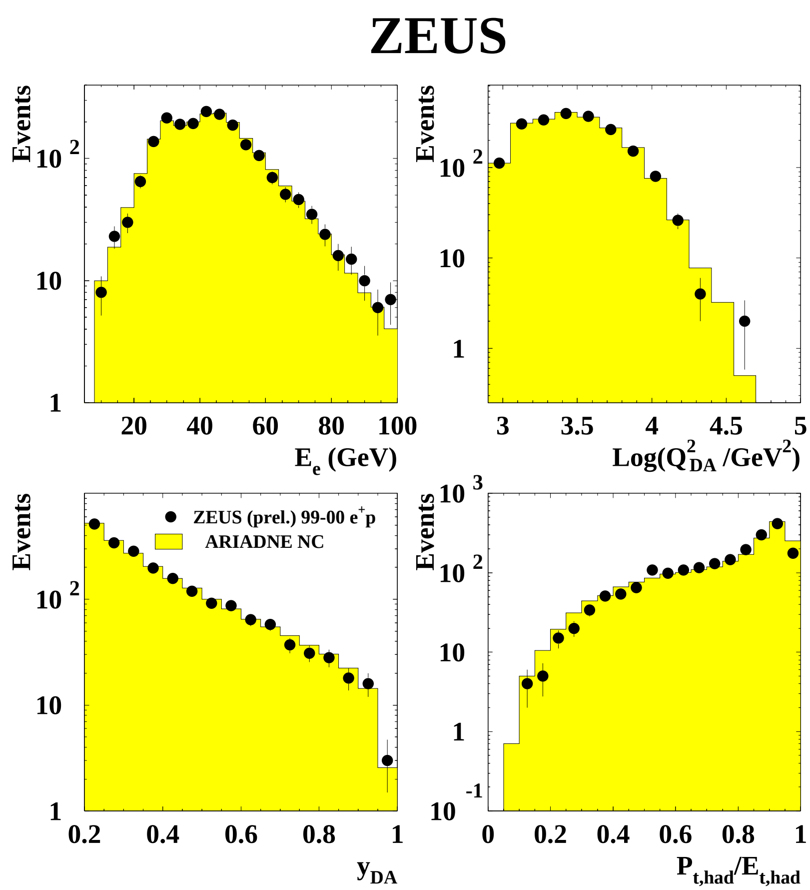

Figure 1: *Comparison between data (dots) and SM MC (histograms) for the energy of the scattered positron* E'_e, $\log_{10}(Q^2_{DA}/GeV^2)$, y_{DA} *and* $P_{t,had}/E_{t,had}$.

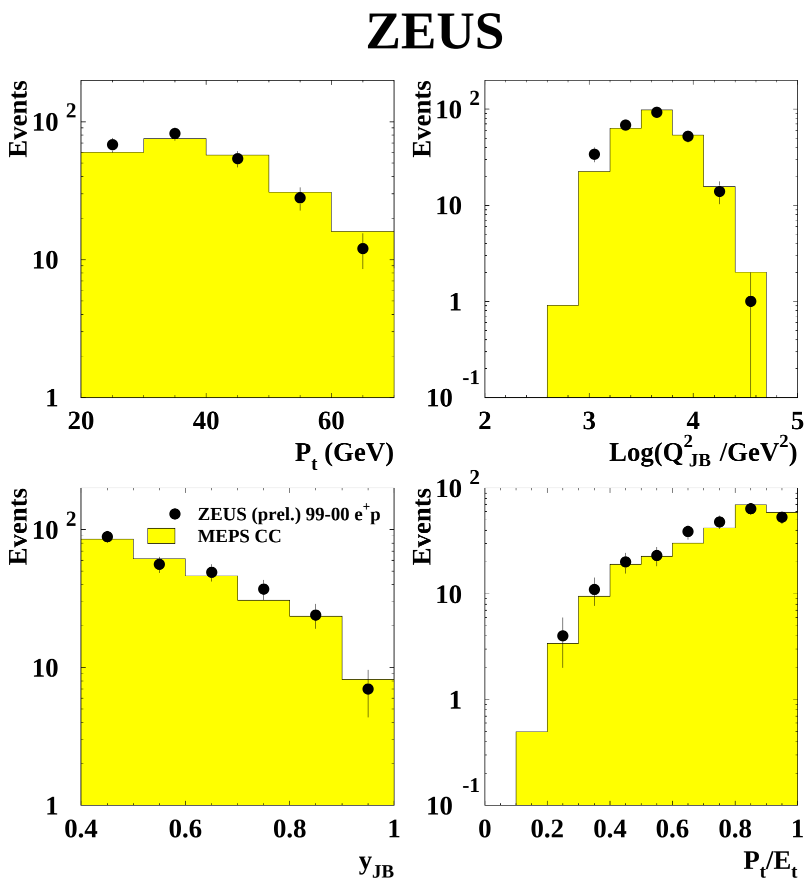

Figure 2: *Comparison between data (dots) and SM MC (histograms) for P_t, $\log_{10}(Q^2_{JB}/GeV^2)$, y_{JB} and P_t/E_t.*

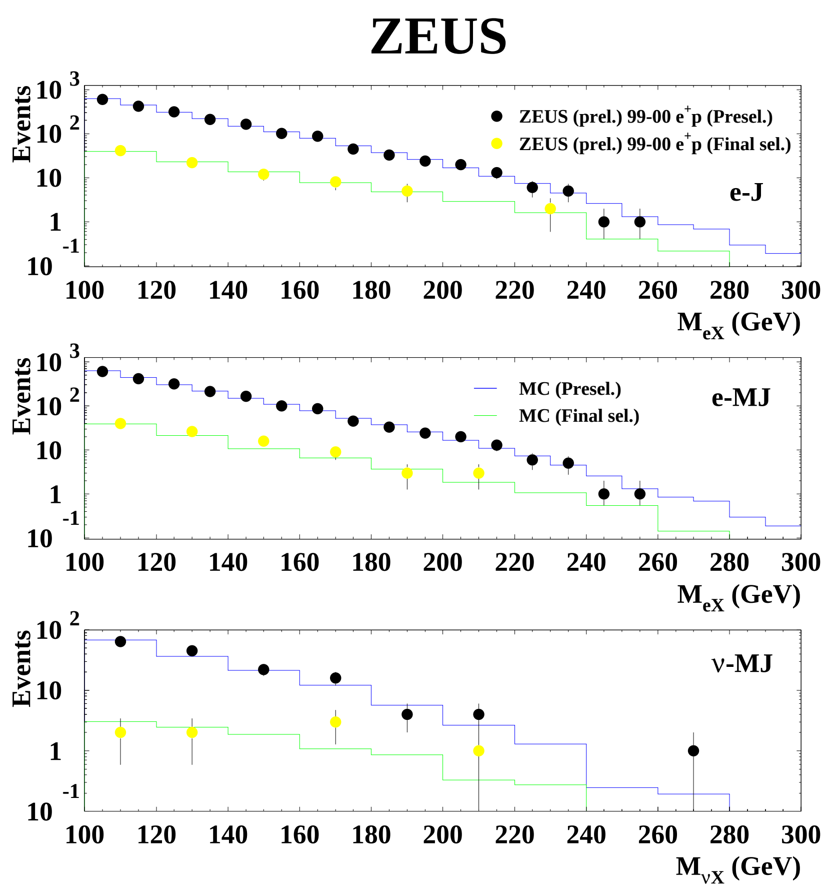

Figure 3: *Comparison between data (dots) and SM MC (histograms) after pre-selection (dark dots and histograms) and final selection (light dots and histograms).*

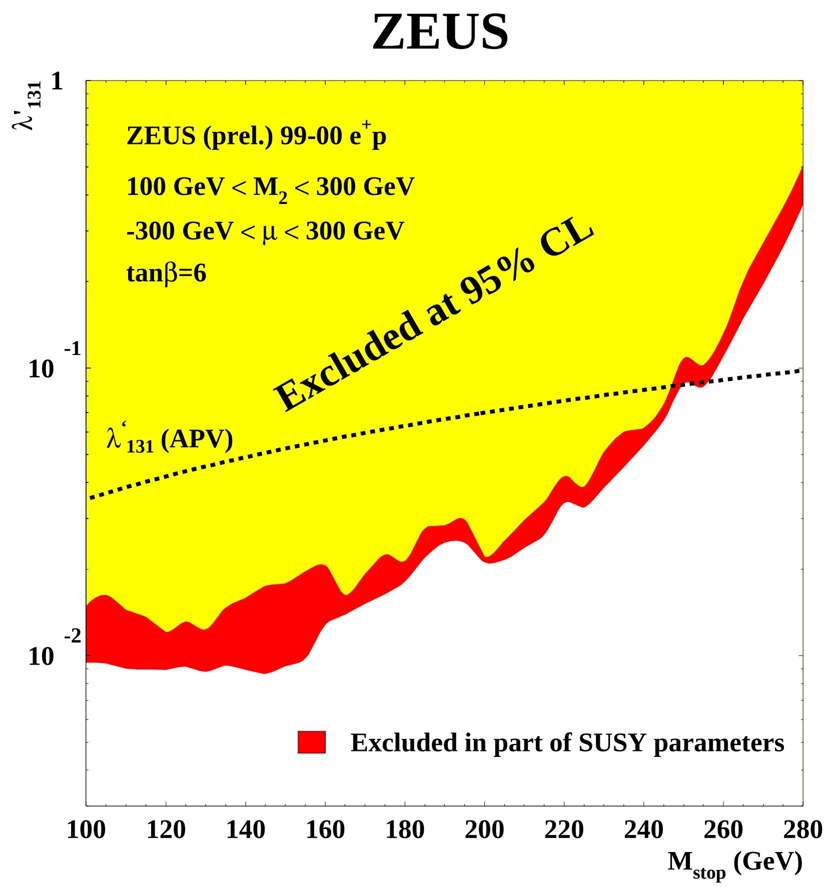

Figure 4: *Limits on λ'_{131} as a function of the stop mass. The light (dark) region is excluded for all (part of the) considered SUSY scenarios. The limit from low-energy APV measurements is also shown.*